Mass limit for the Standard Model Higgs boson with the full LEP I ALEPH data sample

D. Buskulic, I. de Bonis, D. Decamp, P. Ghez, C. Goy, J.P. Lees, A. Lucotte, M.N. Minard, J.Y. Nief, P. Odier, et al.

CERN PPE/96-079
17 June 1996

Mass Limit for the Standard Model Higgs Boson with the full LEP I ALEPH Data Sample

The ALEPH Collaboration*)

Abstract

The reaction $e^+e^- \to HZ^*$ is used to search for the standard model Higgs boson in the $H\nu\bar{\nu}$ and the $H\ell^+\ell^-$ channels. The data sample corresponds to about 4.5 million hadronic Z decays collected by the ALEPH experiment at LEP from 1989 to 1995 at centre-of-mass energies at and around the Z peak. Three candidate events are found in the $H\mu^+\mu^-$ channel, in agreement with the expected background from the electroweak process $e^+e^- \to \ell^+\ell^- q\bar{q}$. This search results in a 95% C.L. lower limit on the Higgs boson mass of 63.9 GeV/c^2.

(Submitted to Physics Letters)

---

*) See next pages for the list of authors

The ALEPH Collaboration

D. Buskulic, I. De Bonis, D. Decamp, P. Ghez, C. Goy, J.-P. Lees, A. Lucotte, M.-N. Minard, J.-Y. Nief, P. Odier, B. Pietrzyk

Laboratoire de Physique des Particules (LAPP), IN^{2}P^3-CNRS, 74019 Annecy-le-Vieux Cedex, France

M.P. Casado, M. Chmeissani, J.M. Crespo, M. Delfino, I. Efthymiopoulos,[1] E. Fernandez, M. Fernandez-Bosman, Ll. Garrido,[15] A. Juste, M. Martinez, S. Orteu, C. Padilla, I.C. Park, A. Pascual, J.A. Perlas, I. Riu, F. Sanchez, F. Teubert

Institut de Fisica d'Altes Energies, Universitat Autonoma de Barcelona, 08193 Bellaterra (Barcelona), Spain[7]

A. Colaleo, D. Creanza, M. de Palma, G. Gelao, M. Girone, G. Iaselli, G. Maggi,[3] M. Maggi, N. Marinelli, S. Nuzzo, A. Ranieri, G. Raso, F. Ruggieri, G. Selvaggi, L. Silvestris, P. Tempesta, G. Zito

Dipartimento di Fisica, INFN Sezione di Bari, 70126 Bari, Italy

X. Huang, J. Lin, Q. Ouyang, T. Wang, Y. Xie, R. Xu, S. Xue, J. Zhang, L. Zhang, W. Zhao

Institute of High-Energy Physics, Academia Sinica, Beijing, The People's Republic of China[8]

R. Alemany, A.O. Bazarko, G. Bonvicini,[23] M. Cattaneo, P. Comas, P. Coyle, H. Drevermann, R.W. Forty, M. Frank, R. Hagelberg, J. Harvey, P. Janot, B. Jost, E. Kneringer, J. Knobloch, I. Lehraus, G. Lutters, E.B. Martin, P. Mato, A. Minten, R. Miquel, Ll.M. Mir,[2] L. Moneta, T. Oest,[20] A. Pacheco, J.-F. Pusztaszeri, F. Ranjard, P. Rensing,[12] L. Rolandi, D. Schlatter, M. Schmelling,[24] M. Schmitt, O. Schneider, W. Tejessy, I.R. Tomalin, A. Venturi, H. Wachsmuth, A. Wagner

European Laboratory for Particle Physics (CERN), 1211 Geneva 23, Switzerland

Z. Ajaltouni, A. Barrès, C. Boyer, A. Falvard, P. Gay, C . Guicheney, P. Henrard, J. Jousset, B. Michel, S. Monteil, J-C. Montret, D. Pallin, P. Perret, F. Podlyski, J. Proriol, P. Rosnet, J.-M. Rossignol

Laboratoire de Physique Corpusculaire, Université Blaise Pascal, IN^{2}P^3-CNRS, Clermont-Ferrand, 63177 Aubière, France

T. Fearnley, J.B. Hansen, J.D. Hansen, J.R. Hansen, P.H. Hansen, B.S. Nilsson, B. Rensch, A. Wäänänen

Niels Bohr Institute, 2100 Copenhagen, Denmark[9]

A. Kyriakis, C. Markou, E. Simopoulou, I. Siotis, A. Vayaki, K. Zachariadou

Nuclear Research Center Demokritos (NRCD), Athens, Greece

A. Blondel, G. Bonneaud, J.C. Brient, P. Bourdon, A. Rougé, M. Rumpf, A. Valassi,[6] M. Verderi, H. Videau[21]

Laboratoire de Physique Nucléaire et des Hautes Energies, Ecole Polytechnique, IN^{2}P^3-CNRS, 91128 Palaiseau Cedex, France

D.J. Candlin, M.I. Parsons

Department of Physics, University of Edinburgh, Edinburgh EH9 3JZ, United Kingdom[10]

E. Focardi,[21] G. Parrini

Dipartimento di Fisica, Università di Firenze, INFN Sezione di Firenze, 50125 Firenze, Italy

M. Corden, C. Georgiopoulos, D.E. Jaffe

Supercomputer Computations Research Institute, Florida State University, Tallahassee, FL 32306-4052, USA [13,14]

A. Antonelli, G. Bencivenni, G. Bologna,[4] F. Bossi, P. Campana, G. Capon, D. Casper, V. Chiarella, G. Felici, P. Laurelli, G. Mannocchi,[5] F. Murtas, G.P. Murtas, L. Passalacqua, M. Pepe-Altarelli

Laboratori Nazionali dell'INFN (LNF-INFN), 00044 Frascati, Italy

L. Curtis, S.J. Dorris, A.W. Halley, I.G. Knowles, J.G. Lynch, V. O'Shea, C. Raine, P. Reeves, J.M. Scarr, K. Smith, P. Teixeira-Dias, A.S. Thompson, F. Thomson, S. Thorn, R.M. Turnbull

Department of Physics and Astronomy, University of Glasgow, Glasgow G12 8QQ,United Kingdom[10]

U. Becker, C. Geweniger, G. Graefe, P. Hanke, G. Hansper, V. Hepp, E.E. Kluge, A. Putzer, M. Schmidt, J. Sommer, H. Stenzel, K. Tittel, S. Werner, M. Wunsch

Institut für Hochenergiephysik, Universität Heidelberg, 69120 Heidelberg, Fed. Rep. of Germany[16]

D. Abbaneo, R. Beuselinck, D.M. Binnie, W. Cameron, P.J. Dornan, A. Moutoussi, J. Nash, J.K. Sedgbeer, A.M. Stacey, M.D. Williams

Department of Physics, Imperial College, London SW7 2BZ, United Kingdom[10]

G. Dissertori, P. Girtler, D. Kuhn, G. Rudolph

Institut für Experimentalphysik, Universität Innsbruck, 6020 Innsbruck, Austria[18]

A.P. Betteridge, C.K. Bowdery, P. Colrain, G. Crawford, A.J. Finch, F. Foster, G. Hughes, T. Sloan, M.I. Williams

Department of Physics, University of Lancaster, Lancaster LA1 4YB, United Kingdom[10]

A. Galla, I. Giehl, A.M. Greene, K. Kleinknecht, G. Quast, B. Renk, E. Rohne, H.-G. Sander, P. van Gemmeren C. Zeitnitz

Institut für Physik, Universität Mainz, 55099 Mainz, Fed. Rep. of Germany[16]

J.J. Aubert,[21] A.M. Bencheikh, C. Benchouk, A. Bonissent, G. Bujosa, D. Calvet, J. Carr, C. Diaconu, F. Etienne, N. Konstantinidis, P. Payre, D. Rousseau, M. Talby, A. Sadouki, M. Thulasidas, K. Trabelsi

Centre de Physique des Particules, Faculté des Sciences de Luminy, IN^2P^3-CNRS, 13288 Marseille, France

M. Aleppo, F. Ragusa[21]

Dipartimento di Fisica, Università di Milano e INFN Sezione di Milano, 20133 Milano, Italy

I. Abt, R. Assmann, C. Bauer, W. Blum, H. Dietl, F. Dydak,[21] G. Ganis, C. Gotzhein, K. Jakobs, H. Kroha, G. Lütjens, G. Lutz, W. Männer, H.-G. Moser, R. Richter, A. Rosado-Schlosser, S. Schael, R. Settles, H. Seywerd, R. St. Denis, W. Wiedenmann, G. Wolf

Max-Planck-Institut für Physik, Werner-Heisenberg-Institut, 80805 München, Fed. Rep. of Germany[16]

J. Boucrot, O. Callot, Y. Choi,[26] A. Cordier, M. Davier, L. Duflot, J.-F. Grivaz, Ph. Heusse, A. Höcker, M. Jacquet, D.W. Kim,[19] F. Le Diberder, J. Lefrançois, A.-M. Lutz, I. Nikolic, H.J. Park,[19] M.-H. Schune, S. Simion, J.-J. Veillet, I. Videau, D. Zerwas

Laboratoire de l'Accélérateur Linéaire, Université de Paris-Sud, IN^2P^3-CNRS, 91405 Orsay Cedex, France

P. Azzurri, G. Bagliesi, G. Batignani, S. Bettarini, C. Bozzi, G. Calderini, M. Carpinelli, M.A. Ciocci, V. Ciulli, R. Dell'Orso, R. Fantechi, I. Ferrante, L. Foà,[1] F. Forti, A. Giassi, M.A. Giorgi, A. Gregorio, F. Ligabue, A. Lusiani, P.S. Marrocchesi, A. Messineo, F. Palla, G. Rizzo, G. Sanguinetti, A. Sciabà, P. Spagnolo, J. Steinberger, R. Tenchini, G. Tonelli,[25] C. Vannini, P.G. Verdini, J. Walsh

Dipartimento di Fisica dell'Università, INFN Sezione di Pisa, e Scuola Normale Superiore, 56010 Pisa, Italy

G.A. Blair, L.M. Bryant, F. Cerutti, J.T. Chambers, Y. Gao, M.G. Green, T. Medcalf, P. Perrodo, J.A. Strong, J.H. von Wimmersperg-Toeller

Department of Physics, Royal Holloway & Bedford New College, University of London, Surrey TW20 OEX, United Kingdom[10]

D.R. Botterill, R.W. Clifft, T.R. Edgecock, S. Haywood, P. Maley, P.R. Norton, J.C. Thompson, A.E. Wright

Particle Physics Dept., Rutherford Appleton Laboratory, Chilton, Didcot, Oxon OX11 OQX, United Kingdom[10]

B. Bloch-Devaux, P. Colas, S. Emery, W. Kozanecki, E. Lançon, M.C. Lemaire, E. Locci, B. Marx, P. Perez, J. Rander, J.-F. Renardy, A. Roussarie, J.-P. Schuller, J. Schwindling, A. Trabelsi, B. Vallage

CEA, DAPNIA/Service de Physique des Particules, CE-Saclay, 91191 Gif-sur-Yvette Cedex, France[17]

S.N. Black, J.H. Dann, R.P. Johnson, H.Y. Kim, A.M. Litke, M.A. McNeil, G. Taylor

Institute for Particle Physics, University of California at Santa Cruz, Santa Cruz, CA 95064, USA[22]

C.N. Booth, R. Boswell, C.A.J. Brew, S. Cartwright, F. Combley, A. Koksal, M. Letho, W.M. Newton, J. Reeve, L.F. Thompson

Department of Physics, University of Sheffield, Sheffield S3 7RH, United Kingdom[10]

A. Böhrer, S. Brandt, V. Büscher, G. Cowan, C. Grupen, J. Minguet-Rodriguez, F. Rivera, P. Saraiva, L. Smolik, F. Stephan,

Fachbereich Physik, Universität Siegen, 57068 Siegen, Fed. Rep. of Germany[16]

M. Apollonio, L. Bosisio, R. Della Marina, G. Giannini, B. Gobbo, G. Musolino

Dipartimento di Fisica, Università di Trieste e INFN Sezione di Trieste, 34127 Trieste, Italy

J. Rothberg, S. Wasserbaech

Experimental Elementary Particle Physics, University of Washington, WA 98195 Seattle, U.S.A.

S.R. Armstrong, P. Elmer, Z. Feng,[27] D.P.S. Ferguson, Y.S. Gao,[28] S. González, J. Grahl, T.C. Greening, O.J. Hayes, H. Hu, P.A. McNamara III, J.M. Nachtman, W. Orejudos, Y.B. Pan, Y. Saadi, I.J. Scott, A.M. Walsh,[29] Sau Lan Wu, X. Wu, J.M. Yamartino, M. Zheng, G. Zobernig

Department of Physics, University of Wisconsin, Madison, WI 53706, USA[11]

[1] Now at CERN, 1211 Geneva 23, Switzerland.
[2] Supported by Dirección General de Investigación Científica y Técnica, Spain.
[3] Now at Dipartimento di Fisica, Università di Lecce, 73100 Lecce, Italy.
[4] Also Istituto di Fisica Generale, Università di Torino, Torino, Italy.
[5] Also Istituto di Cosmo-Geofisica del C.N.R., Torino, Italy.
[6] Supported by the Commission of the European Communities, contract ERBCHBICT941234.
[7] Supported by CICYT, Spain.
[8] Supported by the National Science Foundation of China.
[9] Supported by the Danish Natural Science Research Council.
[10] Supported by the UK Particle Physics and Astronomy Research Council.
[11] Supported by the US Department of Energy, grant DE-FG0295-ER40896.
[12] Now at Dragon Systems, Newton, MA 02160, U.S.A.
[13] Supported by the US Department of Energy, contract DE-FG05-92ER40742.
[14] Supported by the US Department of Energy, contract DE-FC05-85ER250000.
[15] Permanent address: Universitat de Barcelona, 08208 Barcelona, Spain.
[16] Supported by the Bundesministerium für Forschung und Technologie, Fed. Rep. of Germany.
[17] Supported by the Direction des Sciences de la Matière, C.E.A.
[18] Supported by Fonds zur Förderung der wissenschaftlichen Forschung, Austria.
[19] Permanent address: Kangnung National University, Kangnung, Korea.
[20] Now at DESY, Hamburg, Germany.
[21] Also at CERN, 1211 Geneva 23, Switzerland.
[22] Supported by the US Department of Energy, grant DE-FG03-92ER40689.
[23] Now at Wayne State University, Detroit, MI 48202, USA.
[24] Now at Max-Plank-Institüt für Kernphysik, Heidelberg, Germany.
[25] Also at Istituto di Matematica e Fisica, Università di Sassari, Sassari, Italy.
[26] Permanent address: Sung Kyun Kwon University, Suwon, Korea.
[27] Now at The Johns Hopkins University, Baltimore, MD 21218, U.S.A.
[28] Now at Harvard University, Cambridge, MA 02138, U.S.A.
[29] Now at Rutgers University, Piscataway, NJ 08855-0849, U.S.A.

1 Introduction

In the minimal standard model, the spontaneous breaking of the $SU(2)_L \times U(1)_Y$ gauge symmetry is achieved at the expense of the introduction of a doublet of complex scalar fields ϕ in self-interaction. As ϕ develops a vacuum expectation value, the W and Z bosons acquire their masses while three of the four initial degrees of freedom are absorbed. A single neutral scalar particle, the Higgs boson H, therefore results with an unspecified mass m_{H}. However, for a given mass of the Higgs boson, the theory predicts its production rates and partial decay widths unambiguously [1].

At centre-of-mass energies near the Z peak, the Bremsstrahlung process $\mathrm{e^+e^-} \rightarrow \mathrm{HZ^*} \rightarrow \mathrm{H\bar{f}f}$, where $\mathrm{\bar{f}f}$ is any lepton or quark pair, is the dominant Higgs boson production mechanism. This process has already been investigated by ALEPH [2] and by the other LEP collaborations [3], via final states with clear signatures and manageable background. Specifically, searches for acoplanar jets accompanied by missing energy, relevant for the $\mathrm{H}\nu\bar{\nu}$ channel, and for energetic lepton pairs in hadronic events, relevant for the $\mathrm{H}\ell^+\ell^-$ channel (ℓ = e or μ), were carried out with the data collected by ALEPH between 1989 and 1992, corresponding to 1,233,000 hadronic Z decays [2]. No events were found and a 95% C.L. lower limit on the standard model Higgs boson mass was set at 58.4 GeV/c^2.

In Ref. [2], the location of the most critical selection cuts was determined following an optimization procedure [4] which consists in minimizing $\overline{\sigma}_{95} = \overline{\mathrm{N}}_{95}/\mathcal{L}$, the average value of the 95% C.L. upper limit on the signal production cross section, with

$$\overline{\mathrm{N}}_{95}(x) = \frac{e^{-b(x)}}{\varepsilon(x)} \left\{ 3.00 + 4.74 b(x) + 6.30 \frac{b^2(x)}{2!} + 7.75 \frac{b^3(x)}{3!} + \cdots \right\}, \qquad (1)$$

as obtained with a large number of Gedanken experiments in the absence of any signal contribution. Here, $\mathcal{L}$ is the total integrated luminosity of the data sample, x is the location of the cut, $\varepsilon(x)$ is the acceptance of the search, obtained from large samples of signal Monte Carlo, and $b(x)$ is the number of background events expected when the cut is applied. This last number is determined from the background Monte Carlo distribution of the variable x after all other cuts have been applied, smoothed and extrapolated so that an analytical representation of $b(x)$ is available.

Since this average upper limit depends on the absolute background level, the cuts are expected to change — namely to be tightened — as more data becomes available. As a result, the number of background events is expected to remain approximately constant, provided that the selection efficiency varies slowly with the cut location. The selection cuts were actually tightened when the two topological searches were updated with the data collected in 1993 [5] and 1994 [6], corresponding to 704,000 and 1,789,000 additional hadronic Z decays, respectively. The improved mass limits obtained from these two updates were 60.3 and 63.1 GeV/c^2 at the 95% confidence level. The same systematic procedure was applied again to the 1995 data, corresponding to a further 781,000 hadronic Z decays, and the overall result is presented in this letter.

2 The ALEPH detector

A detailed description of the ALEPH detector can be found in Ref. [7] and of its performance in Ref. [8].

Charged particles are detected in the central part of the detector, consisting of a vertex detector, a cylindrical drift chamber and a large time projection chamber. A 1.5 T axial magnetic field is provided by a superconducting solenoidal coil. A $1/p_T$ resolution of 6×10^{-4} $(\mathrm{GeV}/c)^{-1}$ is achieved.

Electrons and photons are identified in the electromagnetic calorimeter by their characteristic longitudinal and transverse shower development. The calorimeter, a lead/wire-plane sampling device with fine readout segmentation and a total thickness of 22 radiation lengths at normal incidence, provides a relative energy resolution of $0.18/\sqrt{E}$ (E in GeV).

Muons are identified by their characteristic penetration pattern in the hadron calorimeter, a 1.2 m thick yoke instrumented with 23 layers of streamer tubes, together with two surrounding layers acting as muon chambers. In association with the electromagnetic calorimeter, the hadron calorimeter also provides a measurement of the energy of charged and neutral hadrons with a relative resolution of $0.80/\sqrt{E}$ (E in GeV).

The total visible energy and mass are measured with an energy-flow reconstruction algorithm [8] which combines all of the above measurements, supplemented by the energy detected at low polar angle (down to 24 mrad from the beam axis) by two additional electromagnetic calorimeters which are used primarily for the luminosity measurement. The resolution on the total visible mass M can be parameterized as $\sigma_M = (0.60\sqrt{M} + 0.6)$ GeV/c^2 (M in GeV/c^2) for well contained hadronic final states [8].

Finally, jets originating from b quarks are identified by means of a lifetime b tagging algorithm [9]. This algorithm makes use of a vertex detector, fully operational since 1991, allowing a 50% efficiency to be achieved for $\mathrm{b\bar{b}}$ events, with a purity of 85%.

In the data sample used for the analysis reported here, all major components of the detector were required to be simultaneously operational, and all major trigger logic had to be enabled.

3 The search in the H$\nu\bar{\nu}$ channel

The topology of interest in this section consists of an acoplanar hadronic system accompanied by missing energy, corresponding to the $(\mathrm{H} \rightarrow \mathrm{hadrons})(\mathrm{Z}^* \rightarrow \nu\bar{\nu})$ final state. The analysis makes use, in particular, of the accurate reconstruction of the energy flow in the detector.

3.1 Preselection

The preselection of this topology is unchanged since 1991 [10] and is only briefly recalled here. It is performed on events with a total visible mass smaller than 70 GeV/c^2 and with at least eight charged particle tracks. These tracks must be reconstructed with at least four hits in the time projection chamber, with a polar angle with respect to the beam such that $|\cos\theta| < 0.95$, and must originate from within a cylinder of length 20 cm and radius 2 cm coaxial with the beam and centred at the nominal collision point. In addition, the scalar sum of the charged particle momenta must exceed 10% of the centre-of-mass energy.

In order to avoid energy losses around the beam direction, the fraction of the total visible energy that is measured beyond 30° of that direction is required to exceed 60%, and the energy measured within 12° of the beam axis has to be smaller than 3 GeV. The events are then divided into two hemispheres by a plane perpendicular to the thrust axis, and the angle between the directions of the total momenta measured in the two hemispheres (the acollinearity angle) is required to be smaller than 165°, which removes the bulk of the Z decays into two back-to-back jets.

These cuts are not effective against photon-photon collisions, but they are rejected by requiring a visible mass above 25 GeV/c^2 when the total momentum transverse to the beam is smaller than 10% of the centre-of-mass energy. In addition, the invariant masses measured in both hemispheres are required to be larger than 2.5 GeV/c^2. This last cut is also very efficient against the few remaining Z decays into $\tau^+\tau^-$ and against the $\tau^+\tau^-\mathrm{q\bar{q}}$ four-fermion final state with a low mass $\mathrm{q\bar{q}}$ pair.

A large acollinearity might also be caused by an $\mathrm{e^+e^-}$ annihilation into two jets accompanied by a hard initial state radiation. To remove such events, it is required that the angle between the missing momentum direction and the beam axis be larger than 21.8°, and that the angle between the two hemisphere total momentum directions projected onto a plane perpendicular to the beam (the acoplanarity angle) be smaller than 175°.

Although this preselection is aimed at rejecting two-jet events, it is also efficient against three-jet events, when the three jet energies are well measured. However, when at least one of the energies is mismeasured, the directions of the total momentum and of the two hemisphere momenta are affected so that the distributions of the acollinearity and acoplanarity angles are smeared out. The corresponding selection criteria therefore become less effective.

3.2 Update of the search

The update of the acoplanar jet search simply consists in optimizing with Eq. (1) the cuts on the three variables relevant for the rejection of the remaining background, dominated by three-jet events:

- the sum S of the three jet-jet angles obtained when the event is forced to form three jets, designed to reject $e^+e^- \to b\bar{b}g$ events with two semileptonic decays;
- the isolation angle A of the largest cone around the total missing momentum direction containing an energy smaller than 1 GeV, designed against $e^+e^- \to b\bar{b}g$ events in which the energy of one jet is essentially carried away by a neutrino coming from a semileptonic decay, thus rendering uncertain the determination of this jet direction;
- the acoplanarity angle η, against $e^+e^- \to q\bar{q}g$ events accompanied by a hard initial state radiation, possibly with semileptonic decays too. (This angle is tested only when the three jet directions are compatible with the presence of an undetected photon along the beam direction, as indicated in Ref. [2].)

Figures 1, 2 and 3 show the distributions of these three variables when the data from 1989 to 1995 are included, together with the functions $\mathrm{d}b(x)/\mathrm{d}x$ ($x = \mathrm{S}, \mathrm{A}, \eta$) obtained by fitting to decreasing exponential shapes the relevant background Monte Carlo distributions (all cuts being applied but the cut on x). The background Monte Carlo samples corresponding to seven million hadronic Z decays, and consequently the expressions for the functions $b(x)$, are those used in the analysis of Ref. [2]. The overall normalizations are directly taken from the Monte Carlo and scale with the total integrated luminosity.

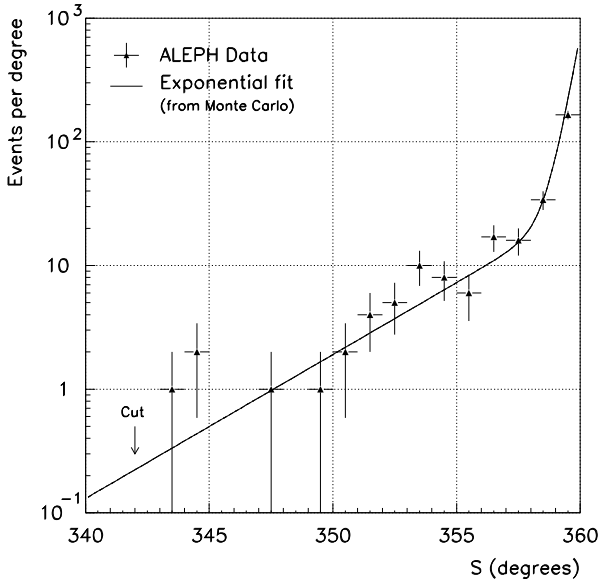

Figure 1: Distribution of the aplanarity S in the data. Also indicated by a solid curve is the result of the (double) exponential fit of $\mathrm{d}b(\mathrm{S})/\mathrm{d}\mathrm{S}$, as obtained from Monte Carlo, with an absolute normalization. The optimized cut location is indicated by an arrow.

Once optimized according to Eq. (1), the cuts on these three variables are set to $\mathrm{S} < 342^\circ$, $\mathrm{A} > 31^\circ$ and $\eta < 159^\circ$. Their evolution with the increase of integrated luminosity between 1992 and 1995 is displayed in Table 1.

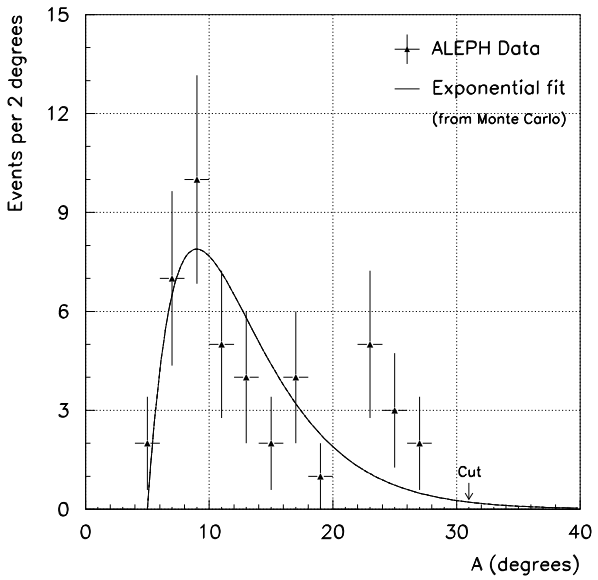

Figure 2: Distribution of the isolation angle A in the data. Also indicated by a full line is the result of the (double) exponential fit of $\mathrm{d}b(\mathrm{A})/\,\mathrm{d}\mathrm{A}$, as obtained from Monte Carlo, with an absolute normalization. The optimized cut location is indicated by an arrow.

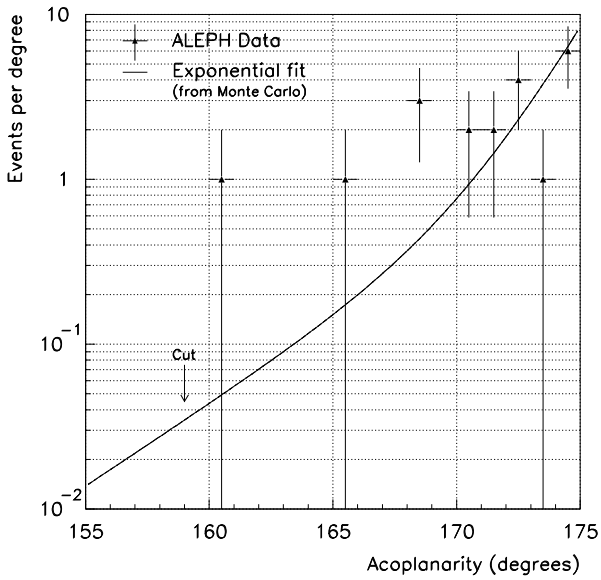

Figure 3: Distribution of the acoplanarity angle η in the data. Also indicated by a full line is the result of the (double) exponential fit of $\mathrm{d}b(\eta)/\,\mathrm{d}\eta$, as obtained from Monte Carlo, with an absolute normalization. The optimized cut location is indicated by an arrow.

Table 1: Cumulative number of hadronic Z decays and optimized value of the cuts on S, A and η, in 1992, 1993, 1994 and 1995. Also indicated is the relative selection efficiency loss for a 60 GeV/c^2 Higgs boson with respect to the previous year.

Year	1992	1993	1994	1995
10^6 Z	1.2	1.9	3.7	4.5
Cut on S	345.0°	343.8°	342.5°	342.0°
Cut on A	25.8°	28.0°	30.5°	31.0°
Cut on η	164°	162°	160°	159°
Efficiency loss (%)	—	4%	5%	1.5%

3.3 Result and systematic studies

Altogether, the updated criteria are expected to select 1.12 ± 0.48 (stat) background events, of which 0.62 ± 0.09 events come from four-fermion processes (0.42 from $e^+e^- \to \nu\bar{\nu}q\bar{q}$ and 0.20 from $e^+e^- \to \tau^+\tau^- q\bar{q}$) and 0.50 ± 0.47 from $e^+e^- \to q\bar{q}$. None are observed in the data, even when the initial 70 GeV/c^2 mass cut is removed. If the cut values optimized for the 1992 integrated luminosity are used instead (see Table 1), six events are found in the data, in agreement with the 4.2 events expected from background processes. The selection efficiency of the $(H \to \text{hadrons})(Z^* \to \nu\bar{\nu})$ final state amounts to $(38.3 \pm 0.2)\%$ and $(29.8 \pm 0.2)\%$ for a 60 and a 65 GeV/c^2 Higgs boson, respectively, to be compared to 43.0% and 33.4% reached with the 1992 selection.

These efficiencies are derived from Monte Carlo and might therefore be affected by some systematic effects in the detector simulation. To study these effects, a control analysis has been performed as in Ref. [8] with multihadronic events containing a very energetic electromagnetic cluster originating either from the radiative process $e^+e^- \to q\bar{q}\gamma$, or from the decay of an energetic π^0 in one of the jets. The selected multihadronic events must have an identified electromagnetic shower (hereafter called a photon) with an energy in excess of 20 GeV and a polar angle with respect to the beam such that $|\cos\theta| < 0.95$. This photon is also required not to be in the vicinity either of the extrapolation of a charged particle track or of a non-instrumented inter-module gap of the electromagnetic calorimeter.

The photon is then removed from the event and the hadronic part is subjected to the preselection described in Section 3.1. After this preselection, the photons of the genuine $q\bar{q}\gamma$ events tend to be isolated from the jets due to the acollinearity and acoplanarity requirements. These events therefore play the rôle of the (mainly) two-jet $H\nu\bar{\nu}$ signal events and can be used to control the selection efficiency. In contrast, for events with an energetic π^0, this procedure selects a three-jet topology, where one of the jets contains the π^0. These events therefore simulate the three-jet background events with at least one jet energy mismeasured, and can be used to control the reliability of the background rejection.

As an example, the distributions of A and S are shown in Fig. 4 for the 5857 events selected in the data and for the simulation with an absolute normalization. The distributions expected from the $e^+e^- \to q\bar{q}\gamma$ signal are then fitted to a simple polynomial, and the three-jet background is parameterized with decreasing exponentials as indicated in Section 3.2.

The survey of these distributions shows that the shape of the signal is well reproduced by the simulation. Since, as expected, these distributions are very similar to those obtained for the $H\nu\bar{\nu}$ signal, this gives confidence in the determination of efficiency of the cuts on S and A, at the level of a percent. (This applies also to the variable η.) In addition, it can be noticed that *(i)* the double exponential shape of the A, S (and η) distributions for the three-jet background, determined with a few tens of simulated $q\bar{q}$ events in Section 3.2, are confirmed with the high statistics π^0 sample; and *(ii)* the cuts on A, S and η at 31°, 342° and 159° are well designed to reject the three-jet background (over 97% of this background is removed this way).

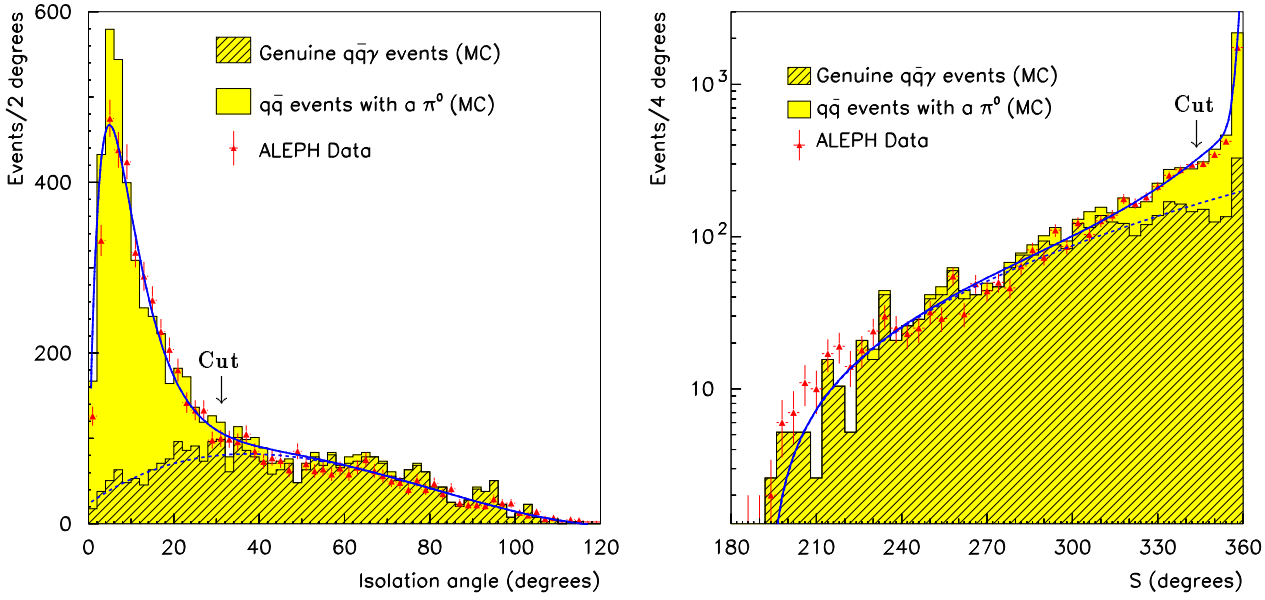

Figure 4: Distribution of A (left) and S (right) for the hadronic events selected with an energetic photon (see text), in the data (triangles with error bars) and from the simulation (histogram), with absolute normalization. The shaded part of the histogram indicates the π^0 contribution and the hatched histogram shows the genuine $q\bar{q}\gamma$ events. The curves indicate the result of a fit of the expected distributions as described in the text.

4 The search in the $H\ell^+\ell^-$ channel

The topology of interest in this section consists of a hadronic system accompanied by a pair of energetic, isolated leptons, corresponding to the $(H \to \text{hadrons})(Z^* \to \ell^+\ell^-)$ final state (ℓ = e or μ). The analysis relies on the lepton identification capabilities of the detector.

4.1 Preselection

As for the H$\nu\bar{\nu}$ channel, the preselection of this topology is unchanged since 1991 [10] and is only briefly recalled here. Only events with at least six charged particle tracks coming from the interaction point and carrying more than 10% of the centre-of-mass energy are considered. Energetic pairs are selected as pairs of oppositely charged particles with individual momenta in excess of 3 GeV/c, with a scalar sum of momenta greater than 20 GeV/c, and with an invariant mass greater than 5 GeV/c^2. Furthermore, the scalar sum of their transverse momenta with respect to the thrust axis of the rest of the event must exceed 15 GeV/c. Events with no such pairs are rejected.

In each pair, at least one of the two particles has to be positively identified as an electron or a muon, according to the strict criteria of Ref. [10]. These criteria are also applied to the second particle except when the track extrapolates to a non-instrumented region of the ECAL for electrons, or of the HCAL for muons. The pairs formed from an electron and a muon are used for systematic studies of the background but are rejected at this level of the search.

To reject $e^+e^- \to b\bar{b}$ events with two semileptonic decays, one of the two leptons is required to be isolated, *i.e.*, no other charged particle must be found inside a cone of 30° half-opening angle around its momentum direction, and less than 1 GeV of neutral energy — apart from identified bremsstrahlung photons as defined in Ref. [10]— must be detected in the same cone.

At this level, $0.0^{+0.3}_{-0.0}$ events are expected from hadronic Z decays, and the main background source is the electroweak four-fermion process $e^+e^- \to \ell^+\ell^- q\bar{q}$, characterized by a topology very close to that of the signal. Repeating the Monte Carlo analysis done in Ref. [11] with `FERMISV` [12], a total of 68.7 events are expected from this source, of which 11.4 have a mass recoiling against the lepton pair in excess of 40 GeV/c^2. A total of 76 events (36 in the He^+e^- channel and 40 in the $H\mu^+\mu^-$ channel) are observed in the data. Among them, 17 events (8 in the He^+e^- channel and 9 in the $H\mu^+\mu^-$ channel) have a mass above 40 GeV/c^2. The probability that 17 events or more are observed when 11.4 are expected is 7%, but this theoretical prediction is expected to be lowered by up to 30% to 50% once gluon radiation, not simulated in FERMISV, is taken into account [11]. Only those events with high recoil mass are considered as candidate events in the present search. Two such events are shown in Fig. 5 and the mass distribution of the whole sample is shown in Fig. 6.

4.2 Update of the search

Given the large number of background events expected, it was noticed in 1993 that the combination of this channel with the acoplanar jets search was bound to eventually degrade, on average, the expected 95% C.L. limit obtained from the H$\nu\bar{\nu}$ channel alone. It was therefore decided, instead of simply removing the H$\ell^+\ell^-$ analysis from the combination, to strengthen its selectivity by adding a requirement on the b quark content of the events [5]. (Only 11% of the standard four-fermion events are expected to be $\ell^+\ell^- b\bar{b}$ events, while over 90% of the hadronic decays of the Higgs boson are expected to be into a $b\bar{b}$ pair.)

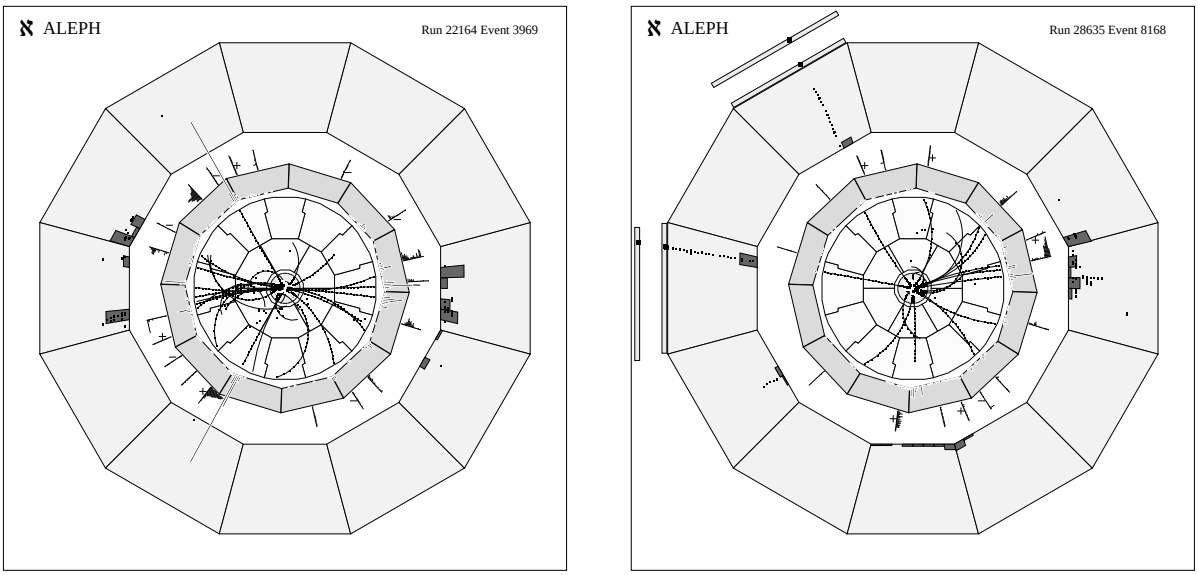

Figure 5: View of the ALEPH detector for a He^+e^- candidate with a recoil mass of 66.0 GeV/c^2 and for a $H\mu^+\mu^-$ candidate with a recoil mass of 49.7 GeV/c^2.

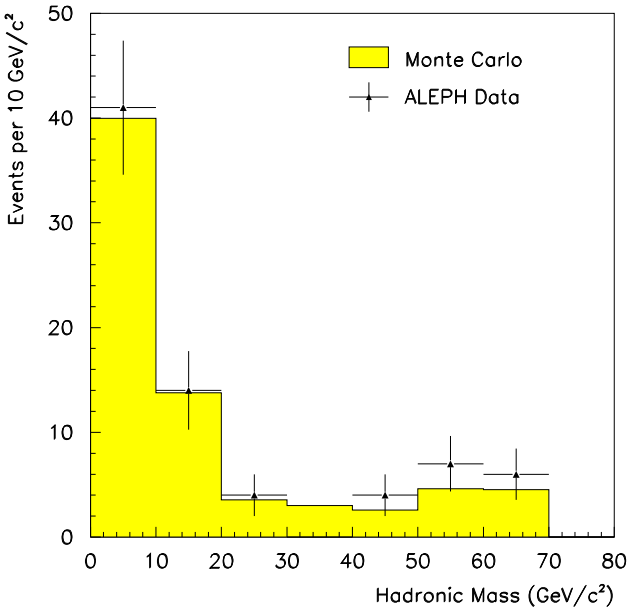

Figure 6: Distribution of the $q\bar{q}$ mass for $e^+e^- \to \ell^+\ell^- q\bar{q}$ Monte Carlo events, with an absolute normalization (shaded histogram), and for the data (triangles with error bars). Here, the $q\bar{q}$ mass is defined either as the mass recoiling against the two leptons for high masses or as the measured hadronic mass for low masses, whichever gives the best resolution.

The b quark content can be quantified with the combined probability P_{uds} for the charged particles of the event to come from the main interaction point [9]. The probability P_{uds} is constructed to be uniformly distributed between 0 and 1 for light quark (u, d, s) events, and peaked at low values for $b\bar{b}$ events. The distribution of P_{uds} for the 17 high mass $H\ell^+\ell^-$ candidates is displayed in Fig. 7 together with the expectation from the electroweak four-fermion process $e^+e^- \to \ell^+\ell^- q\bar{q}$. The update of the analysis consists in optimizing, with Eq. (1), the cut on P_{uds} according to the integrated luminosity.

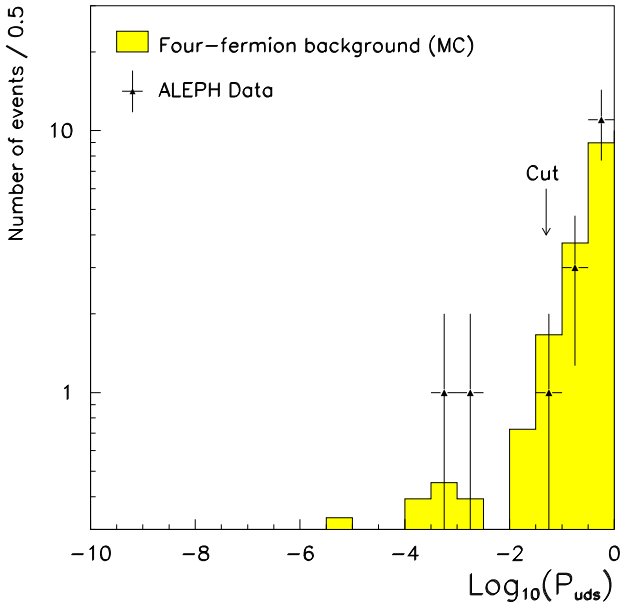

Figure 7: Distribution of $\mathrm{Log}_{10}(P_{uds})$ for $e^+e^- \to \ell^+\ell^- q\bar{q}$ Monte Carlo events, normalized to 17 events (shaded histogram), and for the data (triangles with error bars). The binning is chosen as in Fig. 8. The optimized cut is indicated by an arrow.

For an integrated luminosity corresponding to the whole data sample, the automatic procedure places the optimized cut at $P_{uds} < 0.05$. The cut was set to 0.20 and 0.08 in 1993 [5] and 1994 [6], respectively. The successive losses of efficiency amount to 12%, 8% and 4% with the 1993, 1994 and 1995 optimizations. In addition, the periods during which the vertex detector could not be used (*e.g.* before its installation in 1991) are responsible for another loss of $\sim 7\%$ of the data.

4.3 Result and systematic studies

The updated search is expected to select 2.7 events of which 1.1 are $\ell^+\ell^- b\bar{b}$ events and 1.6 non-b four-fermion events. As can be seen from Fig 7, three events are retained in the data (all in the $H\mu^+\mu^-$ final state), with masses 49.7 ± 0.5, 51.5 ± 0.5 and 66.9 ± 0.3 GeV/c^2. The selection efficiency of the $(H \to \text{hadrons})(Z^* \to \ell^+\ell^-)$ final state amounts to $(39.4 \pm 0.5)\%$ and $(48.1 \pm 0.5)\%$ in the He^+e^- and $H\mu^+\mu^-$ channels, respectively, for a 60 GeV/c^2 Higgs boson.

This is to be compared to the 50.0% and 61.0% reached with the 1992 selection, when no b tagging requirement was applied.

Systematic effects related to the lepton identification have been studied in Ref. [11] with $e^+e^- \to \ell^+\ell^-\gamma$ events. Correction factors of $(-1.7 \pm 0.3)\%$ and $(+0.8 \pm 0.3)\%$ must be applied to the identification efficiency of e^+e^- and $\mu^+\mu^-$ pairs, respectively. The reliability of the simulation of the b tagging has been checked as in Ref. [5] with $q\bar{q}\gamma$ events which contain the same flavour mixture as $q\bar{q}\ell^+\ell^-$ events for high $q\bar{q}$ masses. The selection of the radiative hadronic events follows closely the $H\ell^+\ell^-$ selection, the photon playing the rôle of the lepton pair. Only events with at least four charged particle tracks coming from the interaction point and carrying more than 10% of the centre-of-mass energy are considered. Energetic photons are identified in the electromagnetic calorimeter as in Section 3.3; their energy is required to be greater than 15 GeV and their transverse momentum with respect to the thrust axis of the rest of the event must exceed 10 GeV/c. Events containing an energetic photon from a π^0 (or η) decay are rejected by requiring the photon to be isolated with the same definition as for the lepton isolation.

The remaining π^0 contamination can be further reduced by a factor of two by requiring the major axis of the transverse profile of the electromagnetic shower (expected to be larger for π^0 than for single photons) to be smaller than 2.2 cm. This preselection leads to 2729 events in the data taken between 1991 and 1995, to be compared to the 2643 events predicted by the Monte Carlo, of which 297 are $b\bar{b}\gamma$, 867 $c\bar{c}\gamma$, 333 $s\bar{s}\gamma$, 311 $d\bar{d}\gamma$ and 835 $u\bar{u}\gamma$.

Given its high purity (in excess of 98%), this $q\bar{q}\gamma$ event sample can be directly used to simulate the distribution of the tagging probability P_{uds} expected for $e^+e^- \to q\bar{q}\ell^+\ell^-$. The distribution of P_{uds} is shown in Fig. 8 for the data and for the corresponding Monte Carlo. The fraction of events rejected by a cut on P_{uds} at 0.05 amounts to $(76.7 \pm 0.8)\%$ in the data, to be compared to the Monte Carlo prediction of $(75.9 \pm 0.8)\%$. As can be inferred from Fig. 8, the $(H \to b\bar{b})\ell^+\ell^-$ events are less sensitive to this possible difference between data and simulation. Nevertheless, since the Higgs boson also decays into $c\bar{c}$ and gg with a sizeable branching fraction, it was conservatively assumed that this difference of $(+1.1 \pm 1.4)\%$ is identical for all flavours. The efficiency of this cut as determined from the $H\ell^+\ell^-$ Monte Carlo, 78.8%, must then be corrected by $(-0.3 \pm 0.5)\%$.

5 Combined result of the search

The two topological searches used in this analysis specifically address the $H\ell^+\ell^-$ and the $H\nu\bar{\nu}$ channels, but are also sensitive, although with a low efficiency, to the channels $(H \to$ hadrons$)(Z^* \to \tau^+\tau^-)$ and $(H \to \tau^+\tau^-)(Z^* \to$ hadrons$)$. The number of events expected to be selected by each of the two updated searches in any of the HZ^* final states are shown in Table 2 for different Higgs boson mass hypotheses. The production cross section as well as the decay branching ratios were determined as in Ref. [2] with the `HZHA` generator [13].

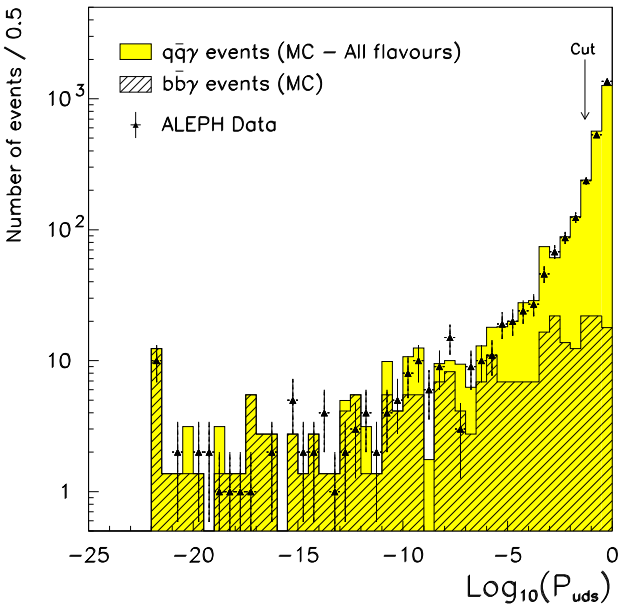

Figure 8: Distribution of the tagging probability P_{uds} for $q\bar{q}\gamma$ events in the data (triangles with error bars) and in the Monte Carlo (shaded histogram). The hatched part of the histogram shows the expected $b\bar{b}\gamma$ contribution.

The various sources of systematic uncertainties on these numbers can be listed as follows.

- An uncertainty of 0.2% is due to the determination of the number of multihadronic events [14] in the data sample.
- The allowed range for the top quark mass, $m_t = 175 \pm 9$ GeV/c^2, obtained from a combination of CDF and D0 data [15], results in an uncertainty of $\pm 0.1\%$ on the ratio of the HZ^* to $q\bar{q}$ cross sections for a Higgs boson mass of 64 GeV/c^2.
- The limited signal Monte Carlo statistics introduces a contribution of 0.2% to the uncertainty.

Table 2: Number of signal events expected to be selected by the acoplanar jet search and by the energetic lepton pair search, for different Higgs boson mass hypotheses.

m_H (GeV/c^2)	Acoplanar Jets	Lepton pairs	Total
50	25.17	8.45	33.62
55	12.23	4.24	16.47
60	5.12	1.87	6.99
65	1.73	0.69	2.42

- The uncertainties related to the selection procedure, the lepton identification and the b tagging were checked directly with the data and contribute an uncertainty of the order of $\pm 1\%$ to the efficiency determination.
- Finally, the ambiguity on the value of the b quark pole mass entering the calculation of the $(H \rightarrow b\bar{b})$ decay partial width introduces a $\pm 1\%$ uncertainty on the corresponding branching ratio. This translates into $\pm 0.7\%$ for the number of events expected.

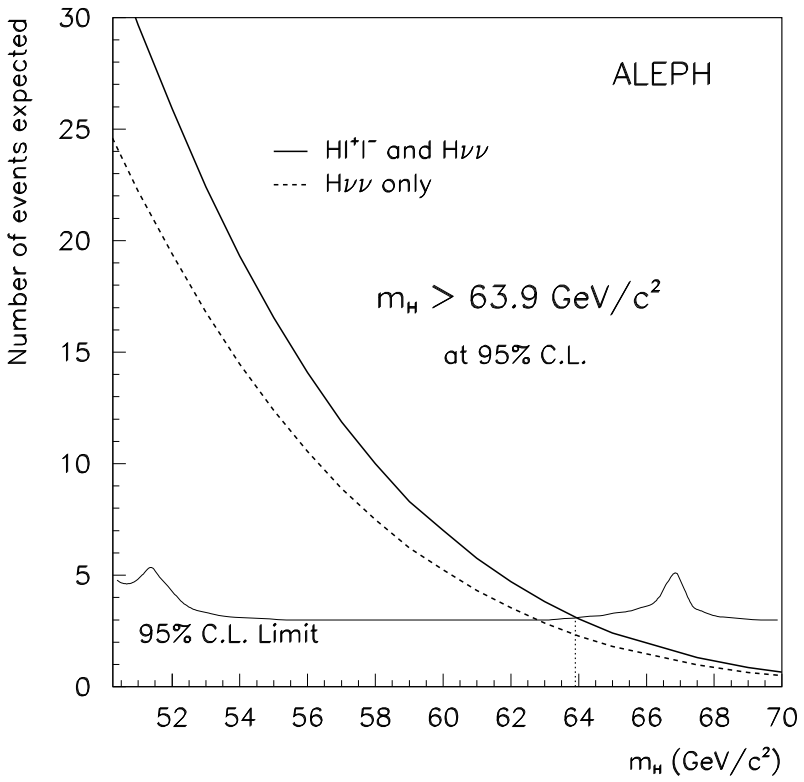

Figure 9: Number of signal events expected to be selected in the acoplanar jet search alone (dashed curve) and in the combination with the lepton search (full curve) as a function of the Higgs boson mass. Also indicated is the 95% C.L. limit on the number of events. The vertical dotted line indicates the 95% C.L. lower limit on the Higgs boson mass.

The overall systematic uncertainty is therefore below 2%. The total number of signal events expected, conservatively reduced by this amount, is presented in Fig. 9 as a function of the Higgs boson mass. No events are observed in the $H\nu\bar{\nu}$ channel (with 1.1 background events expected), and three events are observed in the $H\ell^+\ell^-$ channel, in agreement with the standard model background expectation of 2.7 events. In the derivation of the final result, account is taken of the mass and the mass resolution of the three candidates following the prescription of Ref. [16] (see Fig. 9). This results in an improved 95% C.L. lower limit on the Higgs boson mass of 63.9 GeV/c^2.

Acknowledgements

We wish to thank our colleagues from the accelerator divisions for the successful operation of LEP. We are indebted to the engineers and technicians in all our institutions for their contribution to the excellent performance of ALEPH. Those of us from non-member countries thank CERN for its hospitality.

References

[1] For recent reviews, see:
J.F. Gunion, H.E. Haber, G. Kane, and S. Dawson, *"The Higgs Hunter's Guide"*, Addison-Wesley (1990);
P.J. Franzini et al., *"Z Physics at LEP"*, eds G. Altarelli, R. Kleiss and C. Verzegnassi, CERN 89-08 (1989).

[2] D. Buskulic et al. (ALEPH Coll.), *Phys. Lett.* **B313** (1993) 299.

[3] P. Abreu et al. (DELPHI Coll.), *Nucl. Phys.* **B421** (1994) 2;
O. Adriani et al. (L3 Coll.), *Phys. Lett.* **B303** (1993) 391;
R. Akers et al. (OPAL Coll.), *Phys. Lett.* **B327** (1994) 397.

[4] J.-F. Grivaz and F. Le Diberder, *"Complementary analyses and acceptance optimization in new particles searches"*, LAL preprint # 92-37 (1992).

[5] D. Buskulic et al. (ALEPH Coll.), *"Improved mass limit for the standard model Higgs boson using the ALEPH 1993 Data"*, contribution GLS0568 to the ICHEP, Glasgow, Scotland, July 20-27, 1994.

[6] D. Buskulic et al. (ALEPH Coll.), *"Improved mass limit for the standard model Higgs boson"*, contribution EPS0414 to the IECHEP, Brussels, Belgium, July 27 - August 2, 1995.

[7] D. Decamp et al. (ALEPH Coll.), *Nucl. Instrum. Methods* **A294** (1990) 121.

[8] D. Buskulic et al. (ALEPH Coll.), *Nucl. Instrum. Methods* **A360** (1995) 481.

[9] D. Buskulic et al. (ALEPH Coll.), *Phys. Lett.* **B313** (1993) 535.

[10] D. Decamp et al. (ALEPH Coll.), *Phys. Rep.* **216** (1992) 253.

[11] D. Buskulic et al. (ALEPH Coll.), *Z. Phys.* **C66** (1995) 3.

[12] J. Hilgart, R. Kleiss and F. Le Diberder, *Comput. Phys. Commun.* **75** (1993) 191.

[13] P. Janot, *"The HZHA generator"*, in *"Physics at LEP2"*, Eds. G. Altarelli, T. Sjöstrand and F. Zwirner, CERN 96-01 (1996), Vol. 2, p. 309.

[14] D. Buskulic et al. (ALEPH Coll.), *Z. Phys.* **C60** (1993) 71.

[15] R. Hall (D0 Coll.) and F. Tartarelli (CDF Coll.), talks given at the XXXIst Rencontres de Moriond (1996), to appear in the Proceedings.

[16] J.-F. Grivaz and F. Le Diberder, *Nucl. Instrum. Methods* **A333** (1993) 320.